1 Introduction

- Horizontal axis wind turbine blades extract power from the wind using the aerodynamic forces created on the rotor blades.
- The efficiency of the rotor in extracting the power from the wind is a function of the aerodynamic characteristics of the airfoil sections used in the design of the rotor blades.

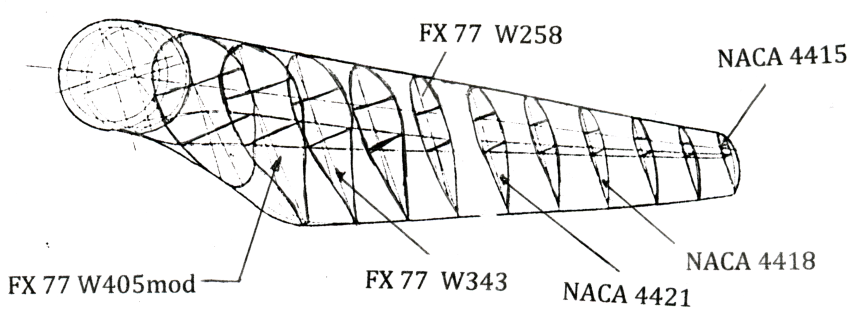

Figure 1: Sketch of a wind turbine showing the different blade shapes across the blade.

2 Airfoil Geometry

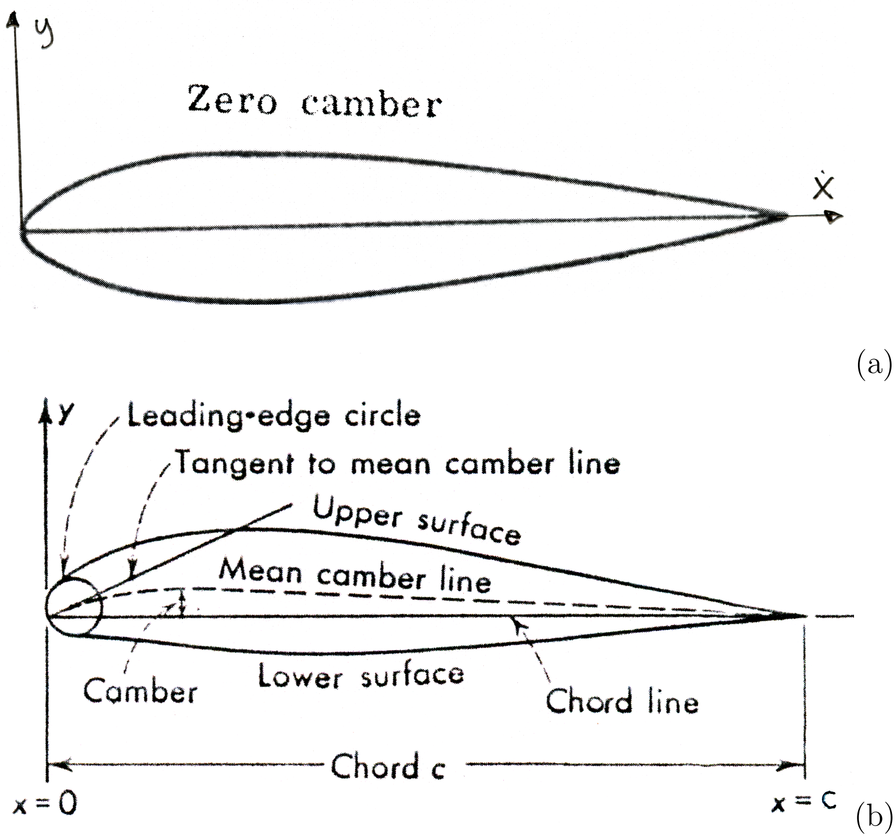

Figure 2: Geometry defining a symmetric airfoil section (a) and a cambered airfoil (b).

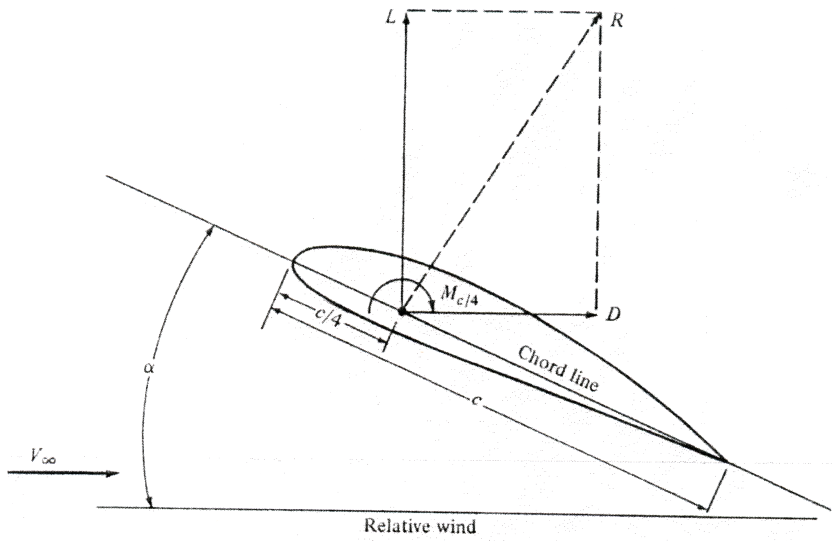

Figure 3: Aerodynamic forces and moment acting on an airfoil.

- The angle of attack, α, is the angle that the freestream velocity makes with the chord line of the airfoil.
- The lift force is perpendicular to the freestream velocity vector
- The drag force is parallel to the freestream velocity vector.
- The pitch moment acts at the quarter-chord location.

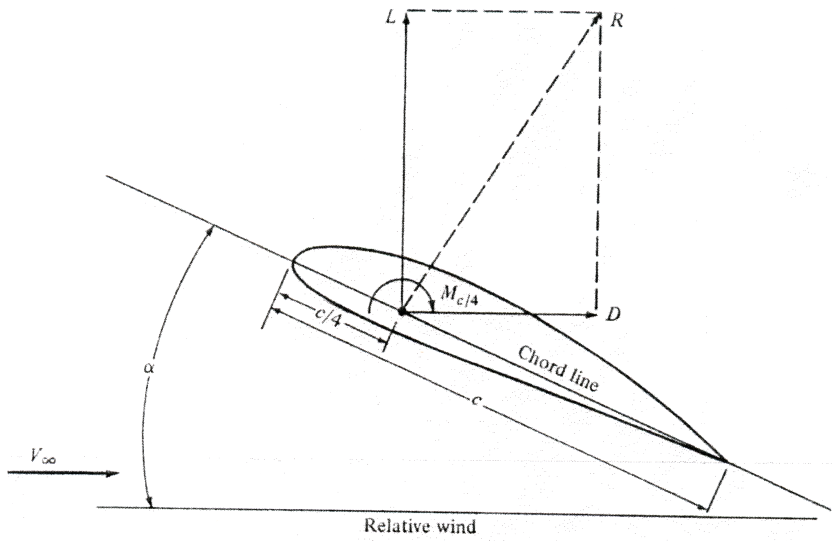

Figure 4: Aerodynamic forces and moment acting on an airfoil.

- Lift coefficient per unit span, C_L

$$C_L = \frac{L}{\frac{1}{2}\rho_\infty V_\infty^2 c}. \tag{1}$$

- The lift coefficient of an airfoil section is a function of angle of attack, Reynolds number, and Mach number, namely

$$C_L = f\left(\alpha, Re, M\right) \tag{2}$$

where

$$Re = \frac{\rho_\infty V_\infty c}{\mu_\infty} \tag{3}$$

and

$$M = \frac{V_\infty}{a_\infty}. \tag{4}$$

- Similarly, for drag coefficient per unit span, C_D and the pitching moment coefficient about quarter-chord location per unit span, $C_{M_{C/4}}$ are

$$C_D = \frac{D}{\frac{1}{2}\rho_\infty V_\infty^2 c} = f\left(\alpha, Re, M\right) \tag{5}$$

and

$$C_{M_{C/4}} = \frac{M}{\frac{1}{2}\rho_\infty V_\infty^2 c^2} f\left(\alpha, Re, M\right). \tag{6}$$

- On a wind turbine rotor, the velocity at any section along the rotor blade is a function of the wind speed, V_∞, and the rotational velocity of the rotor blade, Ωr
  - r is a radial location along the rotor blade
  - Ω is the rotation rate with units of radians/seconds
- The maximum resultant velocity (at the rotor blade tip, $r = R$) is the vector sum of the two velocity components, namely

$$V_R = \sqrt{(V_\infty^2 + (\Omega R)^2} \tag{7}$$

- The cut-out wind speed for modern large wind turbines is around 25 to 30 m/s.
- For typical rotational velocities of the rotor blades, the maximum resultant velocity is well below the Mach numbers where compressibility has any effect on the aerodynamic performance.
- Therefore,

$$C_L = f(\alpha, Re) \tag{8}$$
$$C_D = f(\alpha, Re) \tag{9}$$
$$C_{M_{C/4}} = f(\alpha, Re). \tag{10}$$

3 Airfoil Aerodynamics

- Lift coefficient versus angle of attack for a symmetric airfoil

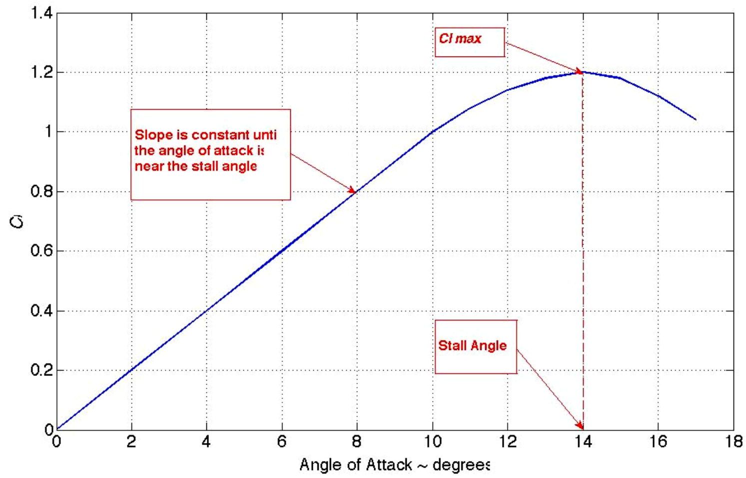

Figure 5: Sample lift coefficient versus angle of attack for a thick symmetric airfoil section.

- Drag coefficient versus angle of attack for a symmetric airfoil

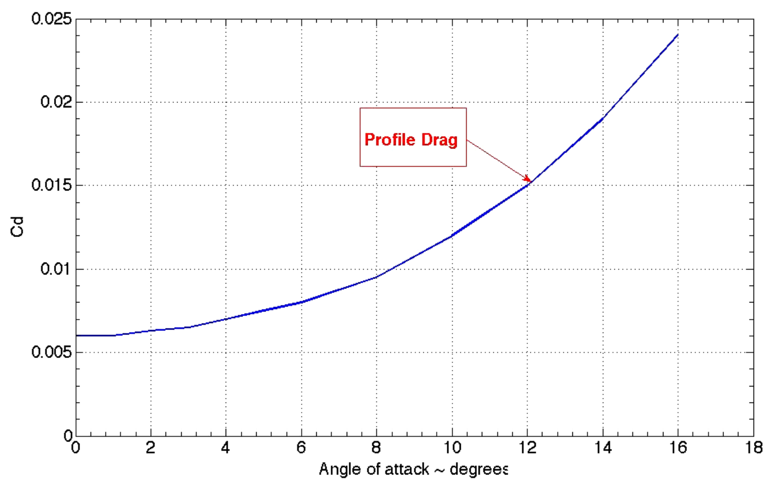

Figure 6: Drag coefficient versus angle of attack for the same airfoil section that produced the lift coefficient versus angle of attack shown in Figure 5.

4 Airfoil Geometry

- The geometry of the airfoil influences its aerodynamic properties.
- In the years from the 1970s to the early 1980s, the wind turbine electric power industry used a number of airfoil designs that were developed by the NACA.
  - The NACA-23XX, NACA-44XX, and NACA-63XXX which are part of the NACA four, five or six digit numbering system used to classify the cross-sectional geometry.
- Example NACA-0006: Symmetric, $t/c = 0.06$

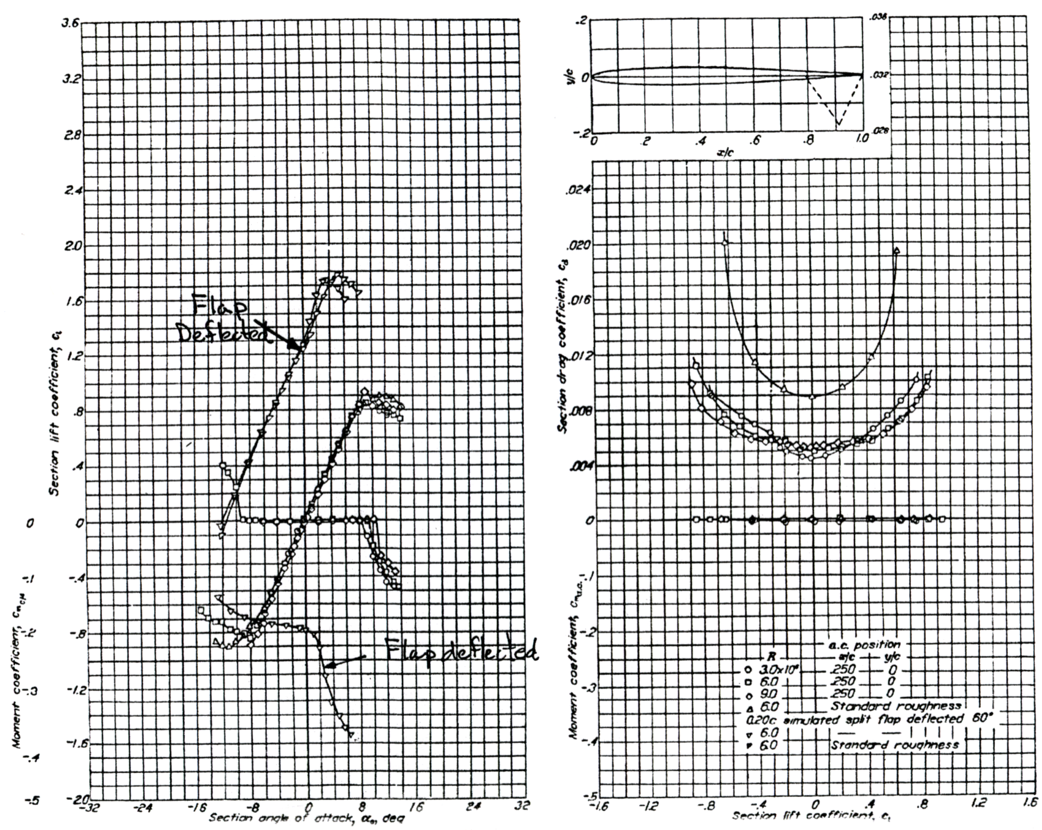

Figure 7: Aerodynamic characteristics of a NACA-0006 airfoil section.

- Example NACA-0012: Symmetric, $t/c = 0.12$

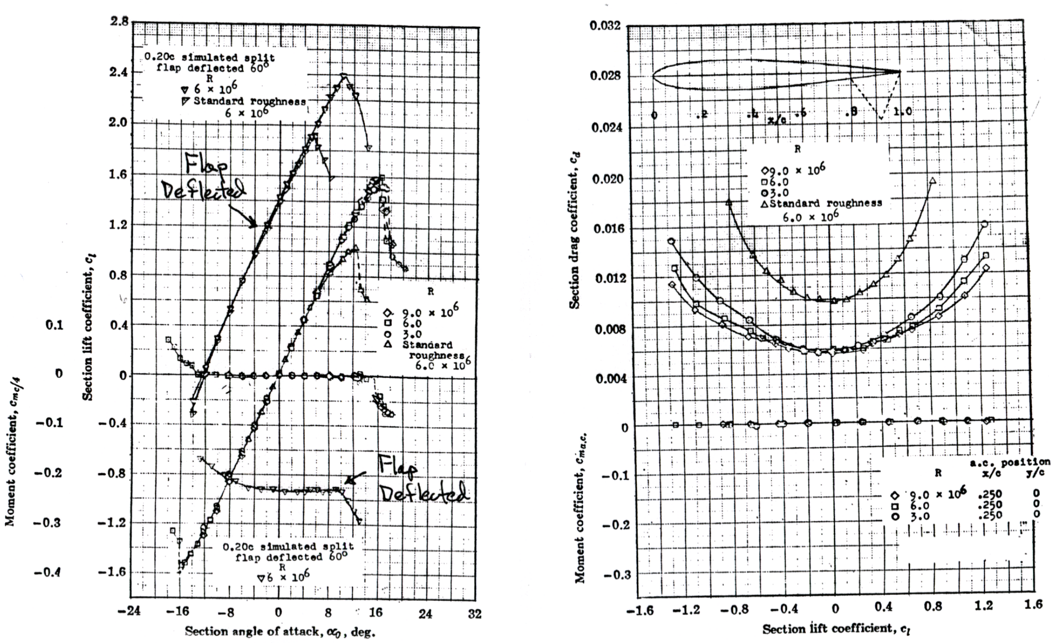

Figure 8: Aerodynamic characteristics of a NACA-0012 airfoil section.

- Example NACA-0012: Cambered, $t/c = 0.12$

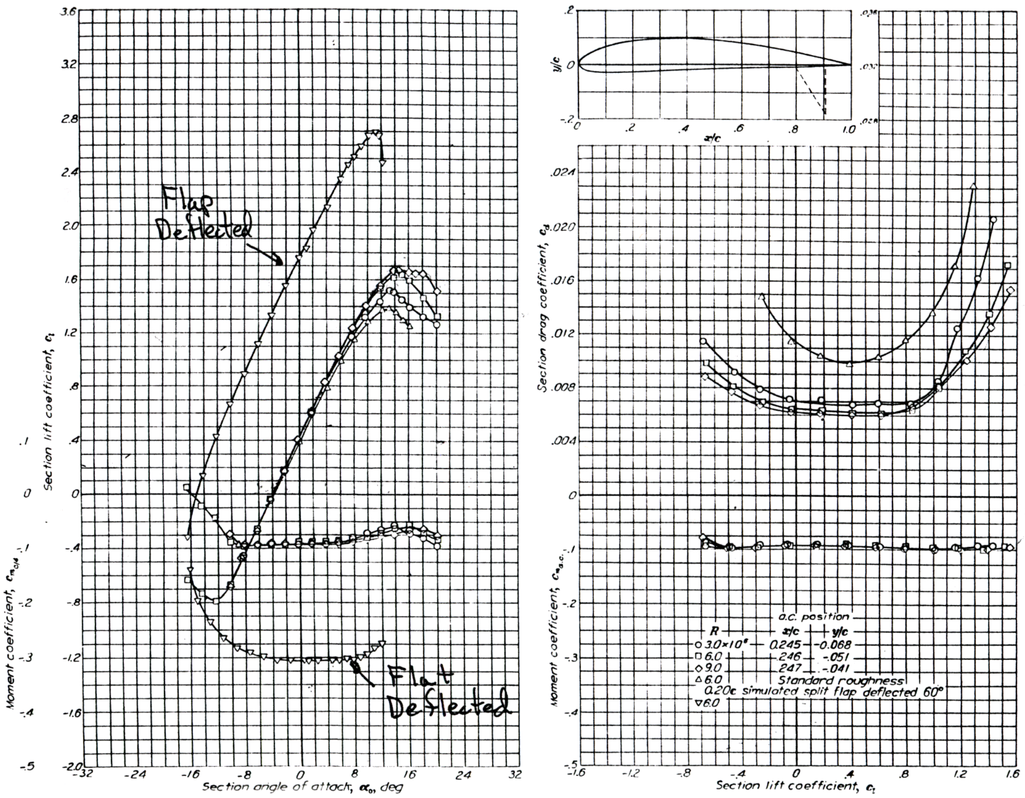

Figure 9: Aerodynamic characteristics of a NACA-4412 airfoil section.

Table 1: Summary of effects of airfoil geometry on aerodynamic characteristics

Reynolds Number	Increasing Reynolds number delays flow separation to a higher angles of attack, increasing $C_{l_{max}}$ and α_s.
Nose Radius	Nose radius increases with increasing t/c. Increasing nose radius increases $C_{l_{max}}$ and α_s.
Airfoil t/c	$C_{l_{max}}$ increases with increasing t/c up to $t/c \simeq 15\%$. Further increases in t/c decrease $C_{l_{max}}$.
Camber	Adding camber shifts the zero lift angle of attack to negative values, and shifts the drag bucket to angles of attack with positive lift, allowing those design lift conditions to have minimum drag.
Surface Roughness	Surface roughness near the leading edge of an airfoil can lead to early stall that results in a lower $C_{l_{max}}$ and increased $C_{d_{max}}$, and as a result a lower $(C_l/C_d)_{max}$.

5 Airfoil Sensitivity to Leading edge Roughness

- Surface roughness near the leading edge of an airfoil can significantly modify the aerodynamic characteristics.

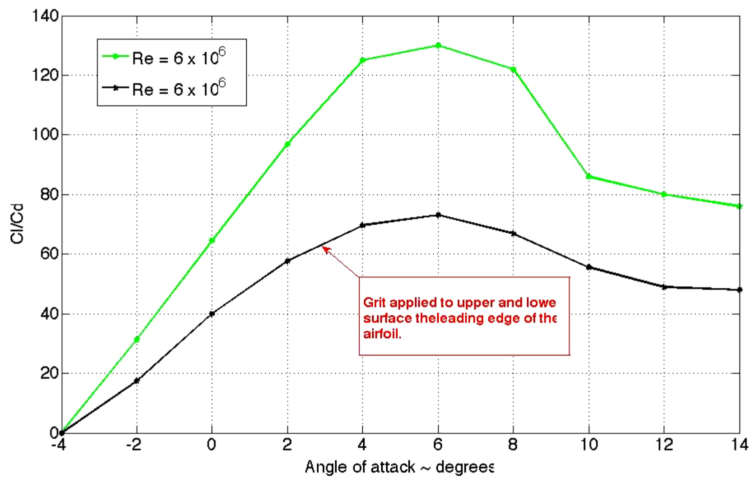

Figure 10: Effect of leading edge roughness on the lift-to-drag ratio versus angle of attack of a NACA-4412 airfoil section.

- Sources of roughness:
  - insect strikes
  - ice and frost
  - abrasion due to wind-borne particles such as sand and dirt
- Led to development of rotor airfoil section shapes that are more tolerant to surface roughness.

6 New Airfoil Designs for the Wind Power Industry

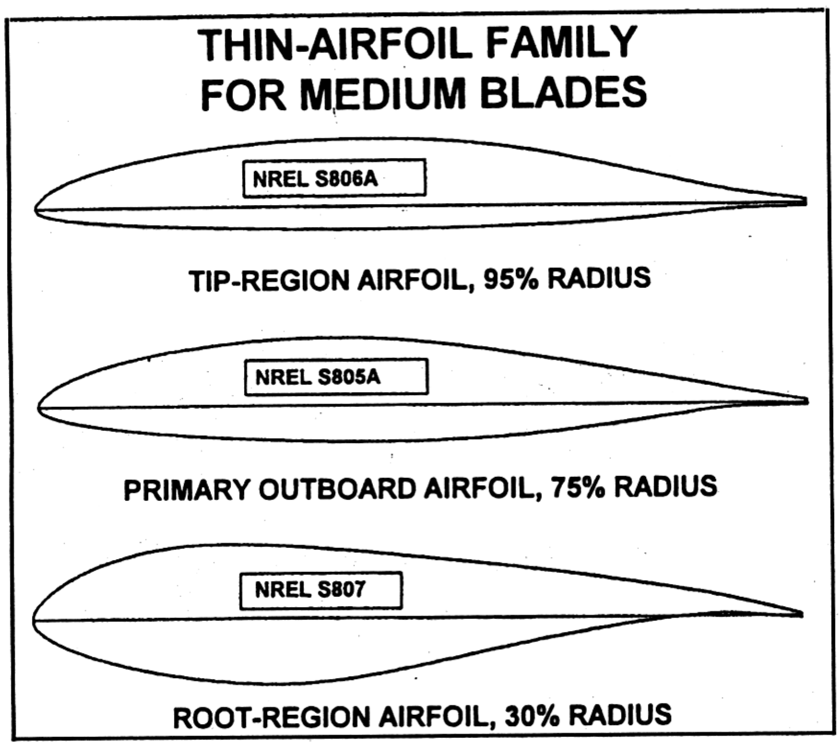

Design Specifications

Airfoil	r/R	Re. No. ($\times10^6$)	t/c	c_{lmax}	c_{dmin}	c_{mo}
S806A	0.95	1.3	0.115	1.1	0.004	-0.05
S805A	0.75	1.0	0.135	1.2	0.005	-0.05
S807	0.30	0.8	0.180	1.4	0.010	-0.10
S808	0.20	0.4	0.210	1.2	0.012	-0.12

Figure 11: NREL thin-airfoil family for use in medium sized wind turbine blades.

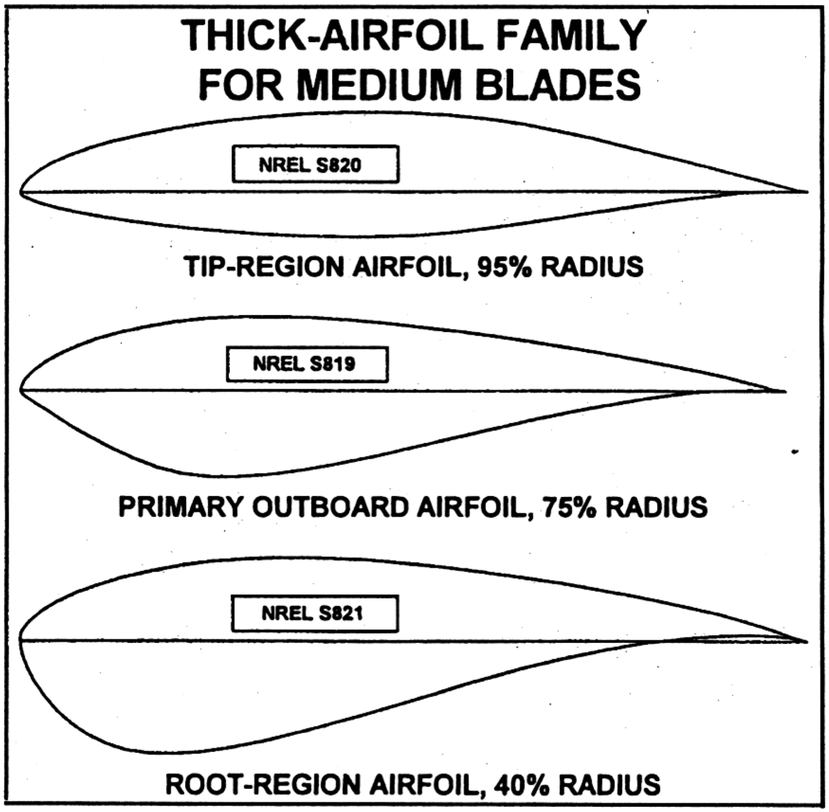

Design Specifications

Airfoil	r/R	Re. No. ($x10^6$)	t/c	c_{lmax}	c_{dmin}	c_{mo}
S820	0.95	1.3	0.160	1.1	0.007	-0.07
S819	0.75	1.0	0.210	1.2	0.008	-0.07
S821	0.40	0.8	0.240	1.4	0.014	-0.15

Figure 12: NREL thick-airfoil family for use in medium sized wind turbine blades.

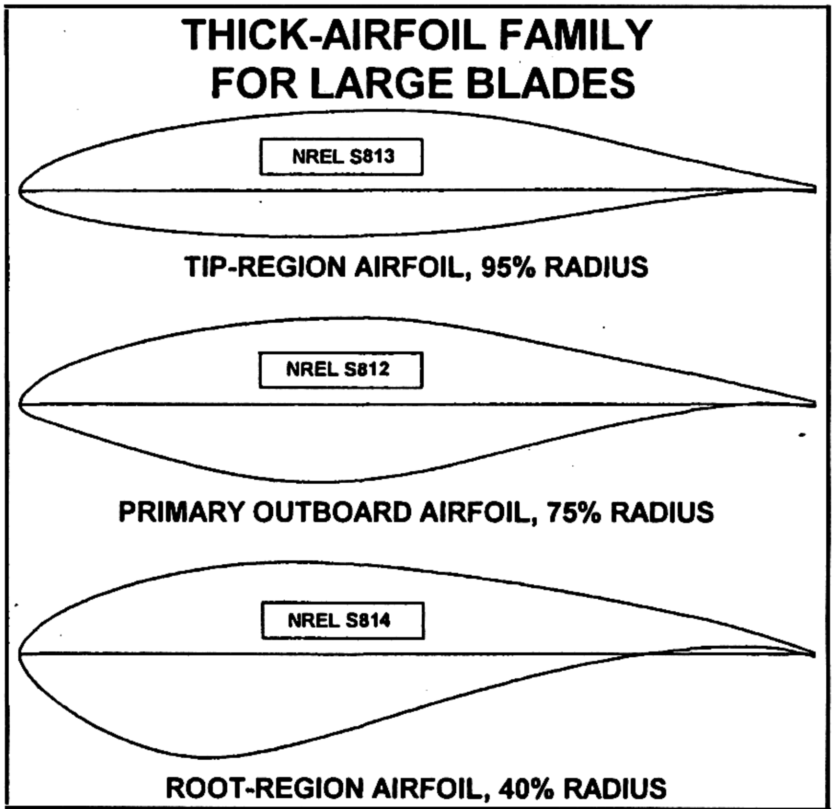

Design Specifications

Airfoil	r/R	Re. No. ($\times 10^6$)	t/c	$c_{l_{max}}$	$c_{d_{min}}$	c_{m_o}
S813	0.95	2.0	0.160	1.1	0.007	-0.07
S812	0.75	2.0	0.210	1.2	0.008	-0.07
S814	0.40	1.5	0.240	1.3	0.012	-0.15
S815	0.30	1.2	0.260	1.1	0.014	-0.15

Figure 13: NREL thick-airfoil family for use in large sized wind turbine blades.

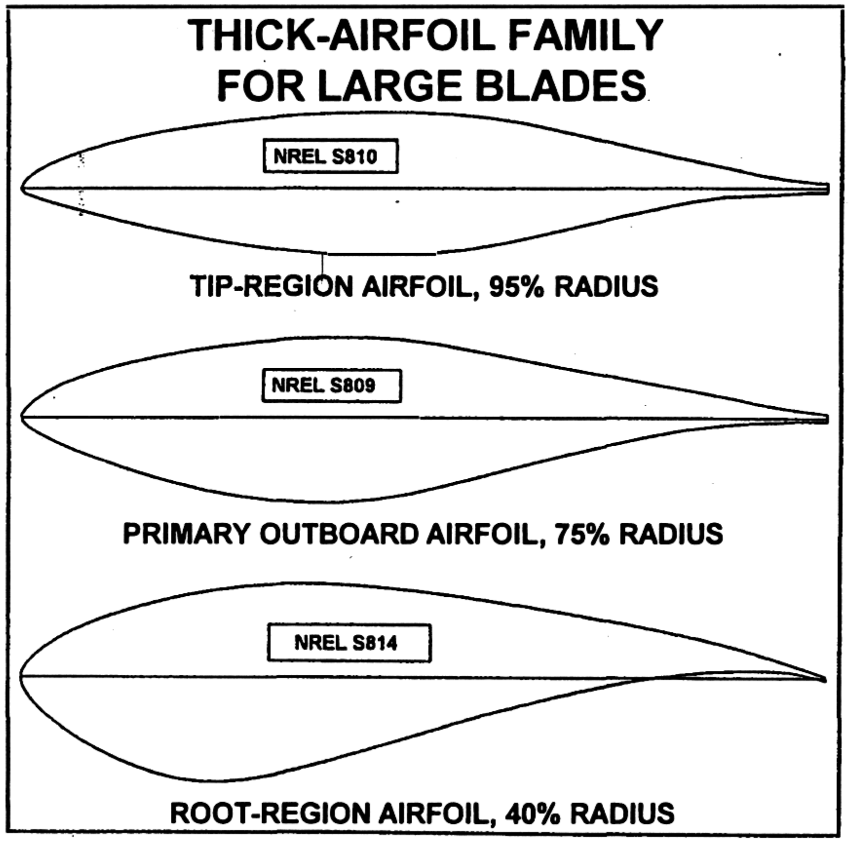

Design Specifications

Airfoil	r/R	Re. No. ($\times 10^6$)	t/c	c_{lmax}	c_{dmin}	c_{mo}
S810	0.95	2.0	0.180	0.9	0.006	-0.05
S809	0.75	2.0	0.210	1.0	0.007	-0.05
S814	0.40	1.5	0.240	1.3	0.012	-0.15
S815	0.30	1.2	0.260	1.1	0.014	-0.15

Figure 14: NREL thick-airfoil family for use in large sized wind turbine blades.

Table 2: Estimated Annual Energy Improvements from NREL Airfoil Series

Turbine Type	Roughness Insensitive $C_{l_{max}}$	Correct Reynolds No.	Low Tip $C_{l_{max}}$	Total Improvement
Stall Regulated	10% to 15%	3% to 5%	10% to 15%	23% to 35%
Variable Pitch	5% to 15%	3% to 5%	-	8% to 20%
Variable RPM	5%	3% to 5%	-	8% to 10%